

Stress dependence of the Eu^{2+} nuclear quadrupole splitting and transferred hyperfine interaction in fluorite crystals*

P. H. Zimmermann[†] and R. Valentin[‡]

II. Physikalisches Institut, Technische Hochschule Darmstadt, D-61 Darmstadt, Germany

(Received 30 October 1974)

We have made electron-nuclear-double-resonance (ENDOR) measurements of the uniaxial stress-induced nuclear quadrupole splitting for Eu^{2+} in BaF_2 , SrF_2 , CaF_2 , and CdF_2 . For stress in the [001] direction the results are in agreement with predictions based on point-charge calculations. In the case of stress along the [111] direction, agreement was achieved only if (i) an anticipated stress-induced dipole contribution to the quadrupole splitting was neglected, and (ii) allowance was made for the local compressibility differing from the bulk compressibility.

I. INTRODUCTION

The investigation of the stress-induced nuclear quadrupole splitting of rare-earth ions in crystalline surroundings with electron-nuclear double resonance (ENDOR), for example, is an useful tool in studying crystalline-field effects. Subjecting a cubic system to uniaxial stress brings about a lowering of the symmetry and therefore a change of the nuclear quadrupole splitting of the rare-earth ion. As there is only one crystalline-field term (A_{20}) involved in this shift, a comparison of experimental results with crystalline-field calculations should give unambiguous information.

The only previous observation of such stress-induced quadrupole splitting was reported by Sroubek *et al.* for $\text{CaF}_2:\text{Eu}^{2+}$ and $\text{MgO}:\text{Mn}^{2+}$ systems.¹ For stress along the [001] axis their results are in full agreement with the point-charge calculation. For stress in the [111] direction one expects a stress-induced electric dipole moment at the anion sites for CaF_2 . Agreement could only be obtained if this contribution was neglected. Differences between local and bulk compressibilities were, however, not considered in the analysis.

To clarify this problem, we have made ENDOR measurements of the nuclear quadrupole splitting with simultaneous application of uniaxial stress on Eu^{2+} -doped BaF_2 , SrF_2 , CaF_2 , and CdF_2 , establishing values in CaF_2 with improved precision. These crystals have the CaF_2 structure and form a series with decreasing lattice constant into which rare-earth ions can easily be incorporated. Much work has been done on these systems. In particular, each of these crystals were investigated by ENDOR measurements in the unstressed case.²⁻⁵

A comparative study of the stress-induced quadrupole shift for all four crystals has the advantage of being independent of the value of the Sternheimer antishielding factor γ_∞ of Eu^{2+} , which has only been calculated for the free Eu^{2+} ion. Such a comparison also leads to information about the local compress-

sibility as differing from the bulk compressibility, which may significantly affect the quadrupole splitting. More detailed information about the local compressibility was obtained by studying the stress dependence of the transferred hyperfine interaction in all four systems with ENDOR.

II. EXPERIMENTAL

The experiments to determine the changes in the nuclear quadrupole splitting were carried out at 4.2 K with stress applied along the [001] and the [111] direction. Measurements of the transferred hyperfine spectrum were carried out with stress applied along the [111] direction. The crystals, nominally doped with 0.005–0.01-mole% Eu^{2+} , were obtained from the Frankfurter Kristallverein, Semielements, and Optovac Corp. To obtain a well-defined surface area the crystals were cut in the form of small elongated prisms with typical dimensions of $1.5 \times 1.5 \times 2 \text{ mm}^3$, the longer edge running parallel to the stress axis. The crystal orientation was carefully checked by Laue backscattering, so that the [001] or [111] axis coincides better than $\pm 0.5^\circ$ with the direction of the external stress.

The samples were mounted between two quartz rods in the center of a tunable TE_{011} circular cavity operating at 24 GHz. Maximal pressure of 1000 kg/cm^2 was applied perpendicular to the static magnetic field through one of the quartz rods driven by a stainless-steel tube which entered the top of the cryostat through an O ring. Four brass rods inside the cavity parallel to its axis formed part of a Helmholtz coil used to generate the rf field. Thus, the static magnetic field and the ENDOR rf field lie in a horizontal plane perpendicular to each other while the microwave magnetic field is in the vertical direction.

The Helmholtz coil formed an inhomogeneity in the coaxial line which was terminated outside the Dewar with a 50- Ω resistance to achieve a matching of the rf power amplifier. A superheterodyne spectrometer operating at 24 GHz with an if of 60

TABLE I. Elastic constants of crystals with fluorite structure (units of 10^{-13} cm²/dyn). Values refer to $T = 4.2$ K. a-c, experimental; d, calculated from room-temperature values.

	s_{11}	s_{12}	s_{44}
BaF ₂ ^a	14.29	-4.48	39.31
SrF ₂ ^b	9.69	-2.61	30.23
CaF ₂ ^c	6.61	-1.42	27.59
CdF ₂ ^d	6.39	-1.74	41.49

^aD. Gerlich, Phys. Rev. **135**, A1331 (1964).

^bD. Gerlich, Phys. Rev. **136**, A1366 (1964).

^cP. S. Ho and A. L. Ruoff, Phys. Rev. **161**, 864 (1967).

^dS. Alterovitz and D. Gerlich, Phys. Rev. B **1**, 4136 (1970).

MHz was used.

In performing the measurements a possible loss of stress due to friction was ruled out, since changing from increasing to decreasing pressure did not result in an observable hysteresis. Care was taken to align the sample with respect to the magnetic field direction. The orientation was checked by observing the transferred hyperfine spectrum on an oscilloscope. Since this spectrum was very sensitive to any misalignment, orientation of better than $\pm 0.1^\circ$ was achieved. In the same manner it was possible to detect a misorientation when stress was applied. Since we were able to correct the crystal orientation in two degrees of freedom, we succeeded in keeping the deviation below $\pm 0.1^\circ$.

III. STRESS-INDUCED NUCLEAR QUADRUPOLE SHIFTS

Application of uniaxial stress to a fluorite-type crystal produces an electric field gradient at the site of the rare-earth impurity. For S-state ions it follows that the main change in the hyperfine interaction is manifested in a change of the quadrupole splitting.

Before discussing our ENDOR measurements of the quadrupole splitting, we briefly present numerical values of the electric field gradient. An evaluation of this gradient has been carried out in Ref. 6 using a point-charge model and summing

over the entire lattice. For stress along the [001] direction, the second-order crystalline-field coefficient was obtained as

$$A_{20} = -0.784(s_{11} - s_{12})T_{\zeta\zeta}e/(\frac{1}{4}a)^3, \quad (1)$$

where e and a denote the magnitude of the electronic charge and the lattice constant, respectively. $T_{\zeta\zeta}$ is the applied stress, ζ denoting the stress axis. Numerical values for the elastic constants s_{ij} are given in Table I. Even though the temperature dependence of the elastic constants is small (less than 10% change between room temperature and 4.2 K), we have used the values appropriate to 4.2 K. For BaF₂, SrF₂, and CaF₂ these are as measured. The values for CdF₂, however, were calculated from room temperature measurements.

For stress along the [111] axis, the monopole contribution to the $l=2$ crystalline-field coefficients is⁶

$$A_{20}(\text{mon}) = 0.261 s_{44} T_{\zeta\zeta}e/(\frac{1}{4}a)^3. \quad (2)$$

There exists, however, also a dipole contribution arising from the electric polarization of the anions. This polarization, which can be shown to be absent for [001] stress from symmetry arguments, is in principle present for [111] stress. Using the method of Ref. 6, we have performed the lattice summation to calculate the stress-induced electric field at the anion site. Assuming an electric polarizability $\alpha = 0.98 \text{ \AA}^3$ for the fluorine anions,⁷ we obtained the following dipole contribution upon another lattice summation:

$$A_{20}(\text{dip}) = 247(\alpha/a^3)A_{20}(\text{mon}). \quad (3)$$

Including 60 000 atoms resulted in a convergence to within 2% of this value of the lattice sum. The numerical values of the second-order crystalline-field coefficients obtained in this manner are shown in Table II.

ENDOR measurements of the stress-induced quadrupole shifts were made by saturating a hyperfine line of the $M_S = +\frac{1}{2} \leftrightarrow -\frac{1}{2}$ transition, since this ESR transition does not change its position with applied stress. Greatest accuracy was achieved by investigating the shift of all the ENDOR transitions

TABLE II. Stress-induced $l=2$ coefficient of the crystalline field for stress applied in the [001] and [111] directions [in units of 10^{-13} ($e/\text{\AA}^3$)/(dyn/cm²)]. For stress in the [111] direction the monopolar as well as the dipolar contributions arising from the pressure-induced electric dipoles at the anion sites are listed.

		BaF ₂	SrF ₂	CaF ₂	CdF ₂
Stress parallel to [001]	$A_{20}/T_{\zeta\zeta}$	-3.951	-3.163	-2.472	-2.611
Stress parallel to [111]	$A_{20}/T_{\zeta\zeta}(\text{mon})$	2.755	2.588	2.827	4.431
	$A_{20}/T_{\zeta\zeta}(\text{dip})$	2.799	3.211	4.197	6.857

with the spectrometer tuned in turn to each of the hyperfine lines. Systematic errors due to sample properties were checked (and found to be negligible) by repeating each measurement with a second sam-

ple.

The data for stress along the [001] and [111] direction were interpreted in terms of the following spin Hamiltonian²

$$\mathcal{H} = [A(\text{Eu})\vec{S} + A'(\text{Eu})\vec{S}^3] \cdot \vec{I}(\text{Eu}) - g_n(\text{Eu})\mu_N \vec{H}_0 \cdot \vec{I} + \frac{B(\text{Eu})}{2S(2S-1)2I(2I-1)} [3I_z^2 - I(I+1)][3S_z^2 - S(S+1)] + Q'(\text{Eu})[I_z - I(I+1)]. \quad (4)$$

Here the (Eu) indicates that measurements were carried out on ^{151}Eu or ^{153}Eu isotopes. The z axis is the direction of the static magnetic field. The ζ axis is the direction of external stress, which is perpendicular to the static magnetic field in our apparatus.

By observing the ENDOR lines due to the $m_I = +\frac{1}{2} \leftrightarrow -\frac{1}{2}$ nuclear transition, no change of the coupling constants A or A' could be detected up to the highest available pressure. The stress dependence of the other transitions arises from the last term of the spin Hamiltonian. This term is related to the stress-induced $l=2$ coefficient in the following way:

$$Q'(\text{Eu}) = \frac{3eQ(\text{Eu})}{2I(2I-1)} A_{20}(1 - \gamma_\infty), \quad (5)$$

where the quadrupole moments $Q(\text{Eu})$ have been obtained⁸ as

$$Q(^{151}\text{Eu}) = 1.16 \text{ b},$$

$$Q(^{153}\text{Eu}) = 2.92 \text{ b}.$$

The Sternheimer antishielding factor γ_∞ has been calculated for the free ion as $\gamma_\infty = -72.6$.⁹ Utilizing these quantities, we determined the experimental and theoretical values for the quadrupole shift.

A. $T_{\zeta\zeta} \parallel [001]$

With stress applied in the [001] direction, the z axis coincides with the [100] direction. The experimental and the calculated values are listed in Table III. An example of the recorder trace of the hyperfine lines with and without stress is shown in Fig. 1.

B. $T_{\zeta\zeta} \parallel [111]$

Applying stress in the [111] direction, we chose the direction of the static magnetic field (z axis) to be along the $[\bar{1}10]$ axis. With this choice of axis, one could easily correct slight misalignments due to the application of stress by observing the splitting of the transferred hyperfine spectrum. The experimental results together with the calculated values of the monopole contribution and also the sum of the monopole and dipolar contributions are also listed in Table III. Spot checks on several transitions of ^{153}Eu were in agreement with the ^{151}Eu values.

Owing to a relatively low signal to noise ratio, the accuracy of the experimental value for the $\text{BaF}_2: \text{Eu}^{2+}$ system is somewhat lower than in the other three systems. The cause was the relatively small concentration of Eu^{2+} in the BaF_2 samples available to us. This affected the accuracy of the measurements with stress in the [111] direction more seriously than the [001] measurements. In the latter case the signal-to-noise ratio was large enough so that it was not the main source of error.

Comparison of the experimental and the calculated values of the quadrupole shift shows that for stress in the [001] direction the relative agreement among the four systems is better than for stress in the [111] direction. Before discussing these results further, we must consider the problem of the local compressibility at the Eu^{2+} site differing from the bulk compressibility. An investigation of this is possible by using the ENDOR technique to map out the local environment.

TABLE III. Experimental and calculated values for the quadrupole interaction constant of $^{151}\text{Eu}^{2+}$ for stress applied in the [001] and [111] directions in units of $\text{Hz}/(\text{kg}/\text{cm}^2)$.

$^{151}\text{Eu}^{2+}$:		BaF_2	SrF_2	CaF_2	CdF_2
Stress parallel to [001]	$Q'/T_{\zeta\zeta}$ (expt)	-197 ± 8	-153 ± 8	-130 ± 8	-134 ± 8
	$Q'/T_{\zeta\zeta}$ (calc)	-172	-138	-108	-113
Stress parallel to [111]	$Q'/T_{\zeta\zeta}$ (expt)	170 ± 20	105 ± 8	98 ± 6	78 ± 8
	$Q'/T_{\zeta\zeta}$ (calc) ^a	120	112	123	193
	$Q'/T_{\zeta\zeta}$ (calc) ^b	242	252	306	492

^aMonopole contribution only.

^bSum of monopole and dipole contributions.

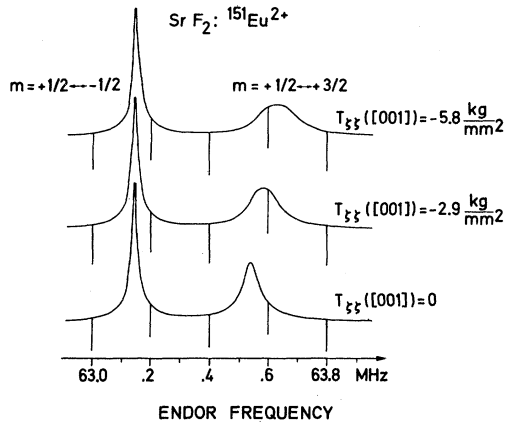


FIG. 1. ^{151}Eu ENDOR spectrum of $\text{SrF}_2:\text{Eu}^{2+}$. The ESR transition $M_S = +\frac{1}{2} \leftrightarrow -\frac{1}{2}$, $m_I = +\frac{1}{2}$ was saturated and only the ENDOR transitions within the $M_S = +\frac{1}{2}$ level are shown. $H_0 = 8,612$ kOe; $\vec{H}_0 \parallel [100]$; $T = 4,2$ K; $\tau = 0,1$ sec. The lower part shows the spectrum without stress; the two spectra at the top were obtained with stress applied in the $[001]$ direction.

IV. STRESS-INDUCED SHIFT OF THE TRANSFERRED HYPERFINE INTERACTION

To measure the local compressibility we have performed ENDOR measurements of the transferred hyperfine interaction under application of uniaxial stress. One expects that a difference between the local and the bulk compressibility would have the largest effect on the shift of the two nearest-neighbor (nn) anions along the $[111]$ axis under application of stress in the $[111]$ direction. These two anions are the only nn that impinge directly upon the Eu^{2+} ion when stressed. All other nn move around the Eu^{2+} ion in a more tangential direction, which is also true for all nn in the case of $[001]$ stress.

The spin Hamiltonian describing the transferred hyperfine interaction has the form³

$$\mathcal{H} = \sum_{i,j,k} [\vec{S} \cdot \vec{A}(F^{i,j,k}) \cdot \vec{I}(F^{i,j,k}) - g_n(F)\mu_N \vec{H}_0 \cdot \vec{I}(F^{i,j,k})]. \quad (6)$$

Here the indices i, j, k denote the position of the fluorine anion with respect to the cubic axes. The tensor A has cylindrical symmetry with the axis of symmetry parallel to the Eu-F lattice vector for the case of equal indices (which includes the nn) where

$$\begin{aligned} A_{ii}^i &= A_s^i + A_d^i + A_p^i, \\ A_{ii}^i &= A_s^i - (A_d^i + A_p^i), \\ A_{pp}^i &= A_{p\pi}^i - A_{p\sigma}^i, \end{aligned}$$

and the index i denotes the ligand shell. A_s arises from the unpaired spin density at the ligand, and

only p_π and p_σ bonding contribute to A_p . The dipole-dipole interaction is given by

$$A_d = g g_n \mu_B \mu_N / R^3. \quad (7)$$

By neglecting the terms S_+ and S_- the ENDOR transition frequencies are shown as given by Baker and Hurrell³

$$\begin{aligned} h\nu(\theta, i) &= \{ [-g_n \mu_N H_0 + A_s^i + (A_p^i + A_d^i)(3 \cos^2 \theta - 1)M_S]^2 \\ &\quad + 9 \sin^2 \theta \cos^2 \theta (A_p^i + A_d^i)^2 M_S^2 \}^{1/2}, \end{aligned} \quad (8)$$

where θ is the angle between the bond axis and the external magnetic field.

Under application of uniaxial stress these frequencies will shift corresponding to the changes in A_s^i and in $A_p^i + A_d^i$. Since the estimated shift is very small, the best chance of successful measurement is with those ligands whose frequency separation from the nuclear Zeeman frequency is largest. For a certain fractional change in the transferred hyperfine coupling constants, one obtains the largest possible absolute shift with those lines.

For our experimental geometry this is the case for the two nn ligands lying on the $[111]$ stress axis, the static magnetic field being in the (111) plane. For the transition frequency of these two ligands we obtain

$$h\nu = -g_n \mu_N H_0 - (A_s - A_p - A_d)M_S. \quad (9)$$

It was not possible to perform measurements of this shift with $\vec{H}_0 \parallel [110]$, since for this direction there exist four equivalent nn ligands with $\theta = \frac{1}{2}\pi$. Choosing $\vec{H}_0 \parallel [11\bar{2}]$ removed this difficulty. In this case only the two nn lying on the $[111]$ stress axis have an angle $\theta = \frac{1}{2}\pi$. The experimental results for the frequency shift of the two ligands are given in Table IV.

An example of a recorder trace of the transferred hyperfine lines with and without stress is shown in Fig. 2.

To interpret the frequency shift in terms of the displacement of the two nn one can use two approaches. As A_d is the largest contribution, in a first approximation one neglects the stress dependence of A_s and A_p . The displacement of the two nn fluorine ions lying on the $[111]$ axis can be calculated from the measured frequency shift using Eq. (7). In a better approximation one can also take into consideration the dependence of A_s and A_p on the Eu-F separation. This can be estimated from the change in A_s and A_p when going from $\text{BaF}_2:\text{Eu}^{2+}$ to $\text{CaF}_2:\text{Eu}^{2+}$. Performing an interpolation shows an almost linear dependence of A_s and A_p on the Eu²⁺-F⁻ separation.⁵ For $\text{CdF}_2:\text{Eu}^{2+}$ the dependence is more complicated, so that the change in A_s and A_p cannot be estimated. Table IV shows our estimated values together with the displacement obtained from the bulk compressibility.

The errors shown here come about entirely from the experimental errors.

TABLE IV. Stress-induced frequency shift ($\Delta\nu$) of the ENDOR lines due to the two nearest-neighbor fluorine ions lying on the [111] stress axis and the stress-induced displacements (Δu_F) of these ions.

Ref.	BaF_2	SrF_2	Eu^{2+} -doped CaF_2	CdF_2	
$\frac{\Delta\nu}{T_{zz}}$	19 ± 3	11 ± 3	10 ± 3	8 ± 3	Hz/(kg/cm ²)
$\frac{\Delta u_F^a}{T_{zz}}$	3.98	2.85	2.42	3.39	10^{-6} Å/(kg/cm ²)
$\frac{\Delta u_F^b}{T_{zz}}$	8.89 ± 1.40	3.94 ± 1.08	2.82 ± 0.85	2.14 ± 0.80	10^{-6} Å/(kg/cm ²)
$\frac{\Delta u_F^c}{T_{zz}}$	5.14 ± 0.81	2.76 ± 0.75	2.34 ± 0.70		10^{-6} Å/(kg/cm ²)

^aDisplacement calculated from the elastic constants.

^bDisplacement calculated from the ENDOR frequency shift, assuming that this shift is due only to the change of the point-dipole interaction constant A_d .

^cDisplacement calculated from the ENDOR frequency shift, assuming that this shift is due to the changes of A_s and A_p as well as A_d .

V. DISCUSSION

We first want to focus our attention on the results of the stress-induced shifts of the transferred hyperfine interaction, because these results are a

necessary presupposition for an interpretation of the stress-induced quadrupole shift. First one must consider the effects due to the incorporation of the Eu^{2+} ion into the fluorite lattice. As can be seen from the lattice constants listed in Table V no

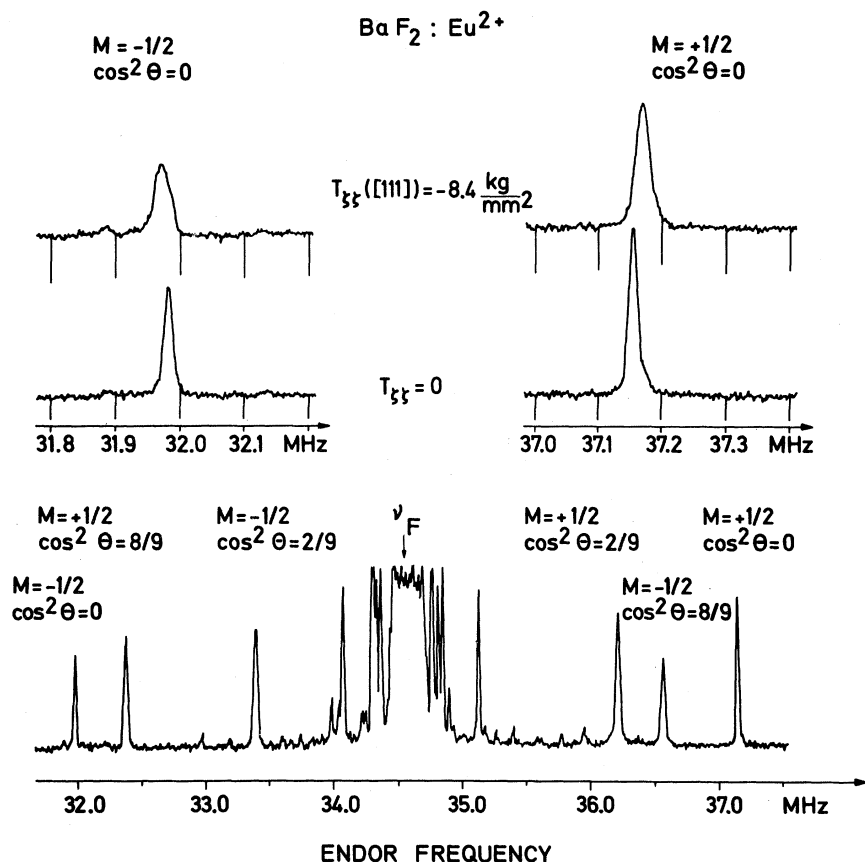


FIG. 2. ^{19}F ENDOR spectrum of $\text{BaF}_2 : \text{Eu}^{2+}$; $H_0 = 8.628$ kOe; $\vec{H}_0 \parallel [11\bar{2}]$; $T = 4.2$ K; $\tau = 0.1$ sec; ν_F is the nuclear Zeeman frequency. The lower part shows the fluorine ENDOR spectrum when saturating the EPR transition $M_S = -\frac{1}{2} \leftrightarrow +\frac{1}{2}$. Expanded view showing the two ENDOR lines due to the two fluorine nuclei lying on the [111] stress axis without stress and with stress applied in the [111] direction.

TABLE V. Lattice constants a_0 (Ref. 10), force constants (Ref. 11), and difference between $\text{Eu}^{2+} - \text{F}^-$ distance and the cation- F^- separation in the undoped lattice (Ref. 5). The values for a_0 refer to 295 K; the change of the lattice constant between 295 K and liquid helium temperature is less than 0.3%.

	BaF ₂	SrF ₂	EuF ₂	CaF ₂	CdF ₂
a_0 (Å)	6.2001	5.7996	5.796	5.46295	5.3880
Force constant (mdyn/nm)	1.34	1.58	...	1.75	1.67
Distortion	-3.9%	+3.5%	+5.9%

distortion of the crystal occurs for the $\text{SrF}_2 : \text{Eu}^{2+}$ system. For $\text{BaF}_2 : \text{Eu}^{2+}$ the nn F^- ions move towards the Eu^{2+} ion, while for CaF_2 and CdF_2 the nn F^- should be pushed outward because the Eu^{2+} ion is "too large" for these lattices. Owing to the weaker force constant as compared to CaF_2 this pushing should be stronger in the CdF_2 system. Under certain assumptions, quantitative values for such displacement can be derived as given in Ref. 5. These values also listed in Table V.

When applying uniaxial stress in the $[111]$ direction one expects the two nn F^- ions lying on the $[11\bar{1}]$ stress axis to be displaced as follows. In the $\text{BaF}_2 : \text{Eu}^{2+}$ the displacement of these two F^- ions should be larger than expected from the bulk compressibility. For the $\text{SrF}_2 : \text{Eu}^{2+}$ system the difference between local and bulk compressibility should be small but no definite conclusion can be drawn. Even though the lattice constants of SrF_2 and EuF_2 are nearly the same, the compressibility of the two systems may differ. Unfortunately no elastic constants for EuF_2 are available. As for $\text{CaF}_2 : \text{Eu}^{2+}$ and $\text{CdF}_2 : \text{Eu}^{2+}$ the nn F^- ions are already pushed away from the Eu^{2+} ion; the displacement of the two nn fluorine ions should be smaller than expected from the bulk compressibility. In the latter case of $\text{CdF}_2 : \text{Eu}^{2+}$ this difference should definitely be large compared to $\text{CaF}_2 : \text{Eu}^{2+}$ since also the force constant between Cd-F ions is weaker.

The experimental results clearly support these ideas. As the displacement derived from the frequency shift under the assumption that only A_d varies with applied stress forms an upper limit for the actual displacement, the value for the $\text{CdF}_2 : \text{Eu}^{2+}$ system establishes that the actual displacement is smaller than predicted with the bulk compressibility outside the limits of error. Thus for $\text{CdF}_2 : \text{Eu}^{2+}$ this is clear evidence that the local compressibility does not equal the bulk compressibility. For $\text{BaF}_2 : \text{Eu}^{2+}$ the values for the displacement obtained under the two approximations are higher than the bulk values, thus also supporting our considerations. For $\text{CaF}_2 : \text{Eu}^{2+}$ and $\text{SrF}_2 : \text{Eu}^{2+}$ the displacement obtained from the measurements agrees with

in the experimental limits of error with the bulk compressibility. No definite conclusion can be drawn, but the tendency among all four systems is in the same direction as predicted.

We were unsuccessful in measuring a shift of the transferred hyperfine lines due to the other six nn for stress in the $[111]$ direction and also in the case for all eight nn for stress in the $[001]$ direction, thus no statement can be made about the displacement from measurements of the transferred hyperfine interaction. According to previous considerations, the difference between the actual and the bulk displacements in this case should be much smaller than in the case of the two nn F^- ions lying along the $[111]$ stress axis.

We now continue with a discussion of the quadrupole shifts. For stress in the $[001]$ direction the experimental and calculated values are in relative agreement for the four systems within the limits of error. Even quantitative agreement may be achieved by allowing for the possibility that the Sternheimer shielding factor is 10% higher than the value calculated for the free Eu^{2+} ion. Therefore, one can rule out local compressibility differing from bulk compressibility, since there is no reason that this difference should vary in the same ratio as the quadrupole shift obtained from the point-charge calculation. Also, contributions due to overlap and covalency effects should be very small because there again is no reason that the change of these contributions should be in the same ratio as the point-charge values.

In comparing the experimental values for the quadrupole shift for stress applied in the $[111]$ direction, the agreement with the values calculated assuming monopole and dipole contributions is poor. (Table III.) Not only is the magnitude too large, but also the change of the calculated shifts shows the wrong tendency when comparing the systems. Better agreement can be achieved considering only the monopole contribution, but the tendency between the four systems does not agree with experiment. However, taking into account the local displacement of the two fluorine ions lying on the $[111]$ stress axis, good agreement is obtained. This is shown in Table VI.

The calculated values of the quadrupole shift, considering the local displacement as obtained from the change in A_d only, tend to overestimate the influence of the different local compressibilities. Therefore, the value for the $\text{BaF}_2 : \text{Eu}^{2+}$ system is high. But it can be seen that the tendency between the four systems is reflected in the correct way. Especially for the $\text{CdF}_2 : \text{Eu}^{2+}$ system there is clear indication that the poor agreement in Table III is caused by a different local compressibility. Taking into consideration the displacement as obtained from the stress-dependent change in A_s , A_p , and

TABLE VI. Stress-induced quadrupole coupling constant for stress applied in the [111] direction neglecting the dipole contribution. Values were calculated taking into consideration the displacement of the two nn fluorine ions lying on the [111] axis as given in Table IV.

Ref.	$^{151}\text{Eu}^{2+}$ -doped			
	BaF ₂	SrF ₂	CaF ₂	CdF ₂
$\frac{Q'}{T_{\text{cr}}}^a$	367 ± 72	179 ± 71	155 ± 74	68 ± 72
$\frac{Q'}{T_{\text{cr}}}^b$	177 ± 41	99 ± 50	113 ± 60	
$\frac{Q'}{T_{\text{cr}}}^c$	170 ± 20	105 ± 8	98 ± 6	78 ± 8

^aDisplacement as given in Ref. b of Table IV was used.

^bDisplacement as given in Ref. c of Table IV was used.

^cThe experimental values are shown for comparison [all units in Hz/(kg/cm²)].

A_d , the agreement with experiment improves even more.

The contribution of the two nn anions lying along the [111] stress axis to the quadrupole shift is of comparable magnitude but of opposite sign to the contribution of the rest of the lattice. The relative experimental error in the determination of the shift of these anions is thus amplified in the results for the quadrupole shift and results in the error

shown in Table VI. Even though this error is considerable, our above conclusions remain unchanged. The stress-induced quadrupole shift for stress in the [111] direction can be explained by considering only the monopole contribution and a different local compressibility.

The apparent absence of the anion dipole contribution to the electric field gradient remains intriguing. This is particularly surprising for the case of SrF₂, as the Eu^{2+} ion is incorporated almost perfectly in this crystal. A possible explanation may be the fact that the electric field was calculated at the site of the fluorine nucleus. As the electric field changes rapidly over the spacial extent of the F⁻ atom, the induced dipole moment will depend on this change. A small contribution may also arise from the polarizability being affected by covalent bonding as outlined in Ref. 12. However, estimates of this effect obtained by calculating the electric field at the midpoint of the bond show that the sign of the covalency contribution is such as to enhance the contribution of the expected fluorine ionic polarizability.

ACKNOWLEDGMENTS

The authors are indebted to Professor B. Elschner for his interest in this work. Special thanks are due to Dr. Z. Sroubek for valuable discussions and many important suggestions.

*Project of "Sonderforschungsbereich Festkörperspektroskopie Darmstadt/Franfurt," financed by special funds of the Deutsche Forschungsgemeinschaft.

†Present address: State University of New York, Department of Physics and Astronomy, Buffalo, New York 14214.

‡Present address: Forschungsinstitut, Fernmeldetechnisches Zentralamt der Deutschen Bundespost, Darmstadt, Germany.

¹Z. Sroubek, E. Simanek, and R. Orbach, Phys. Rev. Lett. **20**, 391 (1968).

²J. M. Baker and F. I. B. Williams, Proc. R. Soc. A **267**, 283 (1962).

³J. M. Baker and J. P. Hurrell, Proc. Phys. Soc. Lond. **82**, 742 (1963).

⁴R. Valentin, Phys. Lett. A **30**, 344 (1969).

⁵K. Baberschke, Z. Phys. **252**, 65 (1972).

⁶Z. Sroubek, M. Tachiki, P. H. Zimmermann, and R. Orbach, Phys. Rev. **165**, 435 (1968).

⁷M. Tachiki, Z. Sroubek, P. Zimmermann, and M. M. Abraham, J. Appl. Phys. **39**, 977 (1968).

⁸W. Müller, A. Steudel, and H. Walther, Z. Phys. **183**, 303 (1965).

⁹R. P. Gupta and S. K. Sen, Phys. Rev. A **7**, 850 (1973).

¹⁰*Crystal Structure*, edited by R. W. G. Wyckoff (Wiley, New York, 1963), Vol. I.

¹¹P. Denham, G. R. Field, P. L. R. Morse, and G. P. Wilkinson, Proc. R. Soc. A **137**, 55 (1970).

¹²M. Tachiki and Z. Sroubek, J. Chem. Phys. **48**, 2383 (1968).